

Photon Echoes Produced by Switching Electric Fields

A. L. Alexander, J. J. Longdell, M. J. Sellars, and N. B. Manson
*Laser Physics Centre, Research School of Physical Sciences and Engineering,
 Australian National University, Canberra, ACT 0200, Australia.*

We demonstrate photon echoes in $\text{Eu}^{3+}:\text{Y}_2\text{SiO}_5$ by controlling the inhomogeneous broadening of the $\text{Eu}^{3+} {}^7\text{F}_0 \leftrightarrow {}^5\text{D}_0$ optical transition. This transition has a linear Stark shift and we induce inhomogeneous broadening by applying an external electric field gradient. After optical excitation, reversing the polarity of the field rephases the ensemble, resulting in a photon echo. This is the first demonstration of such a photon echo and its application as a quantum memory is discussed.

In the emerging area of quantum information science the ability to store and recall quantum states of light it is highly desirable. To date all proposals to achieve this rely on the mapping of light states onto the states of atom-like systems. In spite of the significant effort that has been directed towards this goal, high fidelity reversible mapping of the state of a light field onto atom-like systems has not yet been demonstrated.

The use of atomic ensembles for quantum memory applications is attractive because it allows strong coupling without the need for the high finesse cavities of earlier proposals [1]. Much attention has been given to using the phenomena of electromagnetically induced transparency (EIT) to build quantum memories using atomic ensembles [2, 3]. EIT has led to some dramatic experimental results including ultra-slow group velocities and light storage in trapped atomic systems [4, 5], atomic vapors [6, 7, 8] and the solid state [9, 10]. While EIT can lead to very slow group velocities it has proven difficult to achieve delays with large time-bandwidth products and without high losses [11]. Low time-bandwidth products for delays make high fidelity light storage using EIT difficult. This is because the time-bandwidth product is a measure of how-many distinct pulses fit inside the delay medium and for high fidelity storage the entire pulse must remain inside the medium as the group velocity is slowly reduced to zero. In this work we explore an alternative ensemble based quantum memory on photon echoes.

Coherent manipulation and storage of classical light states using photon echo techniques dates back to the 1980's [12]. In contrast to EIT based techniques where the required slow group velocities are directly linked to narrow bandwidths, recent photon echo based experiments have demonstrated the ability to store thousands of pulses [13] and do signal processing at gigahertz bandwidths [14]. However there is no way currently known to use a standard photon echo, where the rephasing of the atomic coherence is achieved with an optical π -pulse, in a quantum memory.

In 2001 Moiseev and Kröll [15] published a proposal for a quantum memory based on modified photon echos. Instead of rephasing the atomic coherence with intense optical pulses, it used reversible inhomogeneous broadening. Here we report the first demonstration of photon

echoes produced by reversible inhomogeneous broadening. In this case this is achieved using optical centers in a solid which have a linear stark shift and macroscopic electric field gradients.

A quantum memory based on controlled inhomogeneous broadening can be understood as follows: consider a coherent light pulse entering a medium of two-level atoms. The Hamiltonian for the system is of the form:

$$H = H_{\text{field}} + \sum_n \omega_n \sigma_n^z + d(\sigma_n^+ E(z_n, t) + \sigma_n^- E^\dagger(z_n, t)) \quad (1)$$

Here the σ are Pauli operators and d the transition dipole moment. We assume that the area of the incoming pulse is small and that each individual atom is never driven far from its ground state, enabling the approximation $\sigma_z = -1/2$. Working in this small-pulse regime linearizes the equations of motion allowing simple analytic expressions to be derived. It is also the regime of interest for a quantum memory.

The treatment here is semi-classical but because the equations of motion are linear the results should carry straight over to a fully quantum analysis. Treating the atoms as a continuous field $\sigma_n^-(t) \rightarrow \varphi(\delta, z, t) dz d\delta$ one obtains the following equations of motion:

$$\left(-\frac{\partial^2}{\partial z^2} + \frac{1}{c^2} \frac{\partial^2}{\partial t^2}\right) E(z, t) = \eta \int d\delta g(\delta, z) \frac{\partial^2}{\partial t^2} \varphi(\delta, z, t) \quad (2)$$

$$\frac{\partial}{\partial t} \varphi(\delta, z, t) = -i(\omega_0 + \delta) \varphi(\delta, z, t) + d E(z, t) \quad (3)$$

Here $g(\delta, z)$ describes the atom density as a function of detuning and position. Changing variables by setting

$$E(z, t) = E_f(z, t) \exp(i(kz - \omega_0 t)) \quad (4)$$

$$\varphi(\delta, z, t) = \alpha(\delta, z, t) \exp(i(kz - \omega_0 t)) \quad (5)$$

and assuming that the amplitudes E_f and α are slowly varying functions of both z and t . We obtain

$$2ik \left(\partial_z - \frac{1}{c} \partial_t \right) E_f = \eta \omega_0^2 \int d\delta g(\delta, z) \alpha(\delta, z, t) \\ \partial_t \alpha(\delta, z, t) = -i\delta \alpha(\delta, z, t) + E_f(z, t) \quad (6)$$

If we narrow our focus briefly to the situation where we have a spatially homogeneous system with large inhomogeneous

geneous broadening ($g(\delta, z) = 1$) these have the analytical solution [16]

$$E_f(z, t)z = e^{-\eta z} E_f(0, t - z/c) \quad (7)$$

$$\alpha(\delta, z, t) = e^{(i\delta/c - \eta)z} \int_{-\infty}^t d\tau E_f(0, \tau) e^{i\delta\tau} \quad (8)$$

As it propagates, the optical pulse exponentially decays as the atoms absorb the energy. Because of the inhomogeneous broadening the macroscopic coherence of the atomic ensemble also decays. However the process should not be seen as dissipative, each individual atom has not lost any coherence and the absorption process is reversible as described below. For the experiments we performed the detuning is a function of position and the decay of the field is not exponential. The different spectral components of the input field are absorbed at different positions. However as long light pulse is could be totally absorbed the argument for how the memory works is unchanged.

Defining backwards propagating atomic (β) and optical (E_b) fields via

$$E(z, t) = -E_b(z, t) \exp(i(-kz - \omega_0 t)) \quad (9)$$

$$\varphi(\delta, z, t) = \beta(\delta, z, t) \exp(i(-kz - \omega_0 t)) \quad (10)$$

one arrives at the equations of motion

$$2ik \left(\partial_z + \frac{1}{c} \partial_t \right) E_b(z, t) = \eta \omega_0^2 \int d\delta g(\delta, z) \beta(\delta, z, t) \\ \partial_t \beta(\delta, z, t) = -i\delta \beta(\delta, z, t) - E_b(z, t) \quad (11)$$

Comparing Eqns. (11) with the time reversed versions of (6) it can be seen that the two coincide if the sign of δ is reversed. Thus all that is required to make the pulse come out again as a time reversed copy of itself is to flip the detunings of the atoms and at the same time to apply an phase matching operation such that the value of β after the operation is equal to the value that α was before the operation. As $\beta(\delta, z, t) = \alpha(\delta, z, t) \exp(i2kz)$ this phase matching operation is a position dependent phase shift for the atomic states. This can be achieved by driving from the excited state to an auxiliary ground state with a π pulse and driving back up again with another π pulse such that the wavevector difference is $2k$. These two π pulses can be separated in time and between them the coherence is stored in the hyperfine transitions. Coherence times of many seconds have been demonstrated for hyperfine transitions [17] in rare earth ion doped systems.

In [15] it was proposed that the reversible inhomogeneous broadening be achieved using Doppler broadening in an atomic gas. Since then using impurity ions to achieve this controlled inhomogeneous broadening has been proposed [18] and independent of this work the use of electric field gradients has also been proposed [19].

A theoretical treatment of the general case has also appeared [20].

In order for a quantum memory based on controlled inhomogeneous broadening to be practical it is necessary for the induced broadening to be larger than the unbroadened linewidth of the transition. A further requirement is that the field polarity be switched in a time short compared to the inverse of this linewidth. Here we show that these conditions can be achieved in rare earth ion doped systems by successfully demonstrating a *Stark echo*.

The optical transition used in this experiment was the ${}^7F_0 \rightarrow {}^5D_0$ in ${}^{151}\text{Eu}$, at 579.879 nm in 0.1 at% $\text{Eu}^{3+}:\text{Y}_2\text{SiO}_5$. FIG. 1 shows the hyperfine structure of the two electronic singlet states. The transition was excited with linearly polarized light propagating along the C_2 axis of the crystal, with the polarization chosen to maximize the absorption. The length of the crystal in the direction of propagation was 4 mm. The crystal was cooled to below 4 K in a liquid helium bath cryostat. A quadrupole electric field was applied to the sample using four 10 mm long, 2 mm diameter rods in a quadrupolar arrangement as shown in FIG. 1. Two amplifiers with 1 MHz bandwidth supplied the voltage across the electrodes. These amplifiers had two opposite polarity outputs and voltage rails of ± 35 V. This configuration provided an electric field that varied linearly across the sample in the direction of light propagation with a maximum field gradient of approximately 300 Vcm^{-2} .

The optical setup was essentially the same as in previous work [21, 22, 23]. A highly stabilized dye laser was used with an established stability of better than 200 Hz over timescales of 0.2 s. The light incident on the sample was gated with two acousto-optic modulators (AOMs) in series. These allowed pulses with an arbitrary amplitude and phase envelope to be applied to the sample. A Mach-Zehnder interferometer arrangement with the AOMs and sample in one arm was employed to enable heterodyne detection of the coherent emission from the sample. The overall frequency shift introduced by the AOMs was 51 MHz. The intensity of the beat signal was detected with a photo-diode.

The linear Stark shift for the ${}^7F_0 \rightarrow {}^5D_0$ transition in $\text{Eu}^{3+}:\text{Y}_2\text{SiO}_5$ has not been reported but from a study in YAlO_3 it is expected to be of the order of 35 kHzVcm^{-1} [24]. With the current experimental setup the anticipated Stark-induced spectral broadening was therefore 2 MHz. Although this broadening is large compared to the 122 Hz homogeneous linewidth of the optical transition it is significantly smaller than the inhomogeneous linewidth of our sample which was 3 GHz. To create an optical feature which was narrow compared to the induced broadening, the same optical pumping procedure as used in [22, 23] was employed. This consisted of burning a relatively wide (≈ 3 MHz) spectral hole in the absorption line by scanning the laser frequency. A narrow anti-hole was placed in the middle of this region by applying RF

excitation at 80.7 MHz as well as light at a different frequency. This frequency was given by the combination of ground and excited state hyperfine splittings as shown in FIG. 1. The spectral width of the anti-hole was then reduced by optically pumping, out of resonance, ions more than 12.5 kHz from the center frequency of the anti-hole. The peak absorption of the feature was approximately 40%.

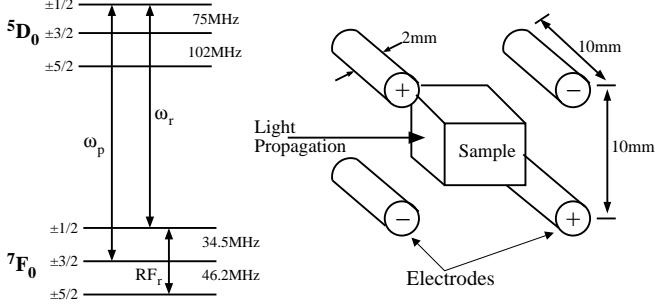


FIG. 1: Energy level diagram of $\text{Eu}^{3+}:\text{Y}_2\text{SiO}_5$ and the arrangement of the electrodes around the sample. The experiment was carried out on the transition labelled ω_p . ω_r and RF_r were used to optically pump the desired ions into the $\pm 3/2$ hyperfine state.

Figure 2 (dotted) shows the free induction decay (FID) resulting from excitation of the spectral feature created as described above, with a $3 \mu\text{s}$ long optical pulse at ω_p . The coherent emission was found to be consistent with that from a 25 kHz wide feature with a top hat profile.

In order to determine the degree of induced broadening, the FID measurement was repeated with an electric field gradient applied after the creation of the spectral feature. By measuring the length of FIDs as the voltage was increased, we estimate the rate of induced broadening to be 42 kHzV^{-1} .

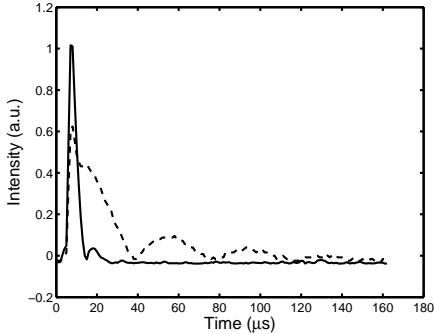


FIG. 2: Broadening of a narrow spectral feature with the electric field gradient. The dotted line shows the FID from a prepared 25 kHz wide feature. The solid line shows how this feature is broadened (and hence its FID is shortened) by the application of the field gradient. The solid trace was taken with $\pm 4.5 \text{ V}$ on the electrodes.

To observe an echo from a feature broadened by apply-

ing 25 V to the electrodes, we excited the feature using a $1 \mu\text{s}$ optical pulse. The polarity of the field was reversed after a time τ , and after a further delay of τ the echo was observed.

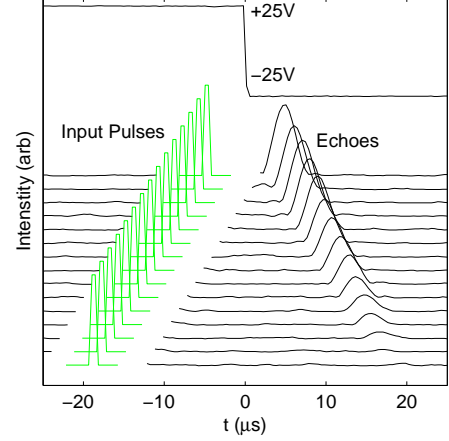


FIG. 3: Stark echoes produced by switching the polarity of the electric field. The top trace is the voltage on the electrodes and the lower traces show the echoes. The signal from the transmitted input pulses saturated the detector and so are only shown schematically. The input pulses were $1 \mu\text{s}$ square shaped pulses and a ratio of 60 dB between the input pulse and the largest echo was measured using a neutral density filter after the sample. The output pulses are broader in time than in input pulses because of the finite bandwidth of the memory. The voltages on the electrodes were $\pm 25 \text{ V}$.

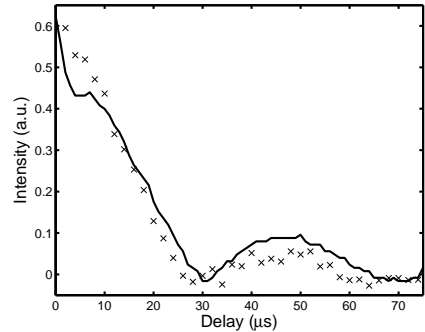


FIG. 4: The solid line represents the FID of a $3 \mu\text{s}$ pulse absorbed over a 25 kHz wide spectral feature. The crosses show the intensity of the Stark echo as a function of total delay. The dephasing mechanism in both cases is the same, the spread of frequencies in the original feature. Therefore the FID provides an envelope for the amplitude of the Stark echoes.

FIG. 3 shows the echoes created using a varying delay between the input pulse and the electric field reversal. The intensity of the echo as a function of the delay is plotted in FIG. 4. From this it can be seen that the envelope of the echo amplitude has the same profile as the FID of the unbroadened spectral feature. The time-

bandwidth product, or the number of distinct pulses that can be stored is four.

The intensity of the echo for a $1.8 \mu\text{s}$ long input pulse as a function of the input pulse intensity is shown in FIG. 5. At the highest input power of 7 mW the pulse area was $\pi/2$. The size of the pulse corresponding to a $\pi/2$ pulse was determined by nutation measurements. The output amplitude is seen to be linear for low input intensities but saturates for pulse areas approaching $\pi/2$.

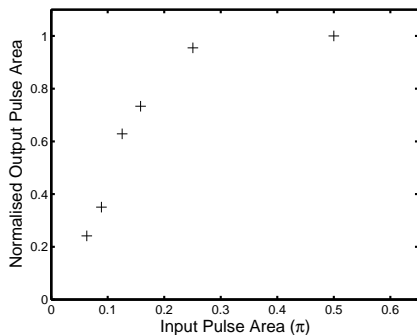


FIG. 5: The energy of the Stark echo as a function of the area of the input pulse. The response is linear until it saturates as the input pulse becomes comparable to a $\pi/2$ pulse.

In these initial experiments the efficiency of the echo was limited by the low level of absorption of the broadened spectral feature. The 40% absorption of the unbroadened line was reduced to 1% on the application of the electric field gradient. For quantum memory applications it will be necessary for the broadened feature to be optically thick.

One way to increase the optical thickness is to increase the interaction length, using longer samples or multi-pass cells. Alternately the absorption could be enhanced by placing the sample an optical cavity.

Another way to increase the optical depth is by increasing the spectral density of the ions. With doped samples it may not be possible to increase the spectral density of the ions by simply increasing the dopant level [25]. This is due to the random strain in the crystal introduced by the dopant ions, producing inhomogeneous broadening that increases linearly with the dopant concentration [26]. An alternative strategy for achieving a high spectral density is to use stoichiometric materials such as $\text{EuCl}_3 \cdot 6\text{H}_2\text{O}$. The spectral density in $\text{EuCl}_3 \cdot 6\text{H}_2\text{O}$ is high due to the high concentration of Eu^{3+} ions and the low level of strain induced broadening.

In conclusion we have shown that it is possible to rephase optical coherence through reversing an external electric field gradient. We demonstrate a time-bandwidth product of four and linear operation at low input intensities. This rephasing using controlled inhomogeneous broadening is the first demonstration of this key effect which has potential applications as a quantum memory.

An elegant aspect of this memory scheme, when compared to other coherence optical memories, is that the only optical excitation is the signal to be stored. The limitation of the current work was the low optical thickness resulting in very low efficiency. Methods for overcoming this limitation were discussed.

The authors would like to thank D. Freeman for his careful reading of the manuscript. This work was supported by the Australian Defence Science and Technology Organisation and the Australian Research Council.

-
- [1] J. I. Cirac, P. Zoller, H. J. Kimble, and H. Mabuchi, *Phys. Rev. Lett.* **78**, 3221 (1997).
 - [2] M. Fleischhauer and M. D. Lukin, *Phys. Rev. Lett.* **84**, 5094 (2000).
 - [3] M. Fleischhauer and M. D. Lukin, *Phys. Rev. A* **65**, 022314 (2002).
 - [4] L. V. Hau, S. E. Harris, Z. Dutton, and C. H. Behroozi, *Nature* **397**, 594 (1999).
 - [5] C. Liu, Z. Dutton, C. H. Behroozi, and L. V. Hau, *Nature* **409**, 490 (2001).
 - [6] M. M. Kash, V. A. Sautenkov, A. S. Zibrov, L. Hollberg, G. R. Welch, M. D. L. Y. Rostovtsev, E. S. Fry, and M. O. Scully, *Phys. Rev. Lett.* **82**, 5229 (1999).
 - [7] D. Budker, D. F. Kimball, S. M. Rochester, and V. V. Yashchuk, *Phys. Rev. Lett.* **83**, 1767 (1999).
 - [8] D. F. Phillips, A. Fleischhauer, A. Mair, R. L. Walsworth, and M. D. Lukin, *Phys. Rev. Lett.* **86**, 783 (2001).
 - [9] A. V. Turukin, V. S. Sudarshanam, M. S. Shahriar, J. A. Musser, B. S. Ham, and P. R. Hemmer, *Phys. Rev. Lett.* **88**, 023602 (2002).
 - [10] J. J. Longdell, E. Fraval, M. J. Sellars, and N. B. Manson, *Phys. Rev. Lett.* **95**, 063601 (2005).
 - [11] A. B. Matsko, D. V. Strekalov, and L. Maleki, *Opt. Express* **13**, 2210 (2005).
 - [12] T. W. Mossberg, *Opt. Lett.* **7**, 77 (1982).
 - [13] H. Lin, T. Wang, and T. W. Mossberg, *Opt. Lett.* **10**, 1658 (1995).
 - [14] K. D. Merkel, R. K. Mohan, Z. Cole, T. Chang, A. Olson, and W. R. Babbitt, *J. Lumin* **107**, 62 (2004).
 - [15] S. A. Moiseev and S. Kroll, *Phys. Rev. Lett.* **87**, 173601 (2001).
 - [16] M. D. Crisp, *Phys. Rev. A* **1**, 1604 (1970).
 - [17] E. Fraval, M. J. Sellars, and J. J. Longdell, *Phys. Rev. Lett.* **95**, 030506 (2005).
 - [18] S. A. Moiseev, V. F. Tarasov, and B. S. Ham, *J. Opt. B* **5**, S497 (2003).
 - [19] M. Nilsson and S. Kroll, *Opt. Comm.* **247**, 393 (2005).
 - [20] B. Kraus, W. Tittel, N. Gisin, M. Nilsson, S. Kroll, and J. Cirac, (2005), quant-ph/0502184.
 - [21] G. J. Pryde, M. J. Sellars, and N. B. Manson, *Phys. Rev. Lett.* **84**, 1152 (2000).
 - [22] J. J. Longdell and M. J. Sellars, *Phys. Rev. A* **69**, 032307 (2004), quant-ph/0208182.
 - [23] J. J. Longdell, M. J. Sellars, and N. B. Manson, *Phys. Rev. Lett.* **93**, 130503 (2004).
 - [24] A. J. Meixner, C. M. Jefferson, and R. M. Macfarlane, *Phys. Rev. B* **46**, 5912 (1992).
 - [25] M. J. Sellars, E. Fraval, and J. J. Longdell, *J. Lumin*

107, 150 (2004).

[26] R. L. Cone, *Personal communication*.